

Reactions of Charged Species in Supercritical Xenon as Studied by Pulse Radiolysis[†]

Richard A. Holroyd* and James F. Wishart

Chemistry Department, Brookhaven National Laboratory, Upton, New York 11973

Masaru Nishikawa

Faculty of Engineering, Kanagawa Institute of Technology, 1030 Shimo-Ogino, Atsugi 243-0292, Japan

Kengo Itoh

Department of Pure and Applied Science, University of Tokyo, Tokyo 153-8902, Japan

Received: January 8, 2003; In Final Form: March 4, 2003

The results of an initial study of the pulse radiolysis of supercritical xenon are reported. In pure xenon, transients are formed that absorb broadly throughout the visible. These transients are assigned to excimer species, Xe_2^* , on the basis of lifetime and kinetic data. The formation of excimers by electron–ion recombination was time-resolved by pulse–probe measurements. The excimers can be quenched by adding small amounts of ethane, which then facilitates detection of other transients by absorption spectroscopy. The added ethane also accelerates the thermalization of electrons and allows measurements of fast reaction rates of thermal electrons. Electron attachment to hexafluorobenzene occurs near the maximum rate at high pressures in xenon–ethane mixtures. The C_6F_6^- anion formed absorbs with a maximum at 500 nm and disappears by second-order kinetics. The mobility of this anion, as measured by conductivity, indicates sizable clusters of solvent around the ion at all pressures, which are of maximum size near critical density. The rate of electron transfer from C_6F_6^- to benzoquinone exceeds $1 \times 10^{11} \text{ m}^{-1} \text{ s}^{-1}$ at most pressures. The rate maximizes near 62 bar at 21.4 °C. A maximum at this pressure is predicted by diffusion. The maximum is related to the increase in cluster size around the anion, which occurs at this pressure.

Introduction

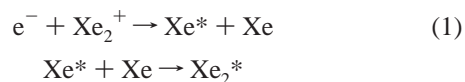
This study was undertaken to further elucidate the physical properties and reactions of charged species in nonpolar supercritical fluids. There have been a few previous studies of the reactions of charged species in such supercritical fluids as a function of pressure. In supercritical CO_2 the reactions of C_2O_4^+ with dimethylaniline and of $(\text{CO}_2)_n^-$ with benzoquinone have been studied and occur near the diffusion-controlled rate.¹ The anionic intermediate in CO_2 also reacts with O_2 , SF_6 , and CCl_4 .² The rate constants exhibit a weak maximum as a function of the density of CO_2 . In supercritical ethane the rate of electron transfer from biphenyl anion to pyrene is reported to be nearly constant over a range of pressures at 35 °C.³

Xenon was selected as a typical nonpolar fluid for this study of ionic reactions by pulse radiolysis for several reasons. It is supercritical at room temperature, it is radiation stable and is transparent throughout most of the spectrum. In addition, the yield of ions is high because electrons produced in ionization processes travel a long way before thermalizing; that is, geminate recombination is unimportant. Also the density is high, 1.11 g/cm³ at the critical density; thus a significant fraction of the electron beam can be stopped in the sample.

The electron beam radiolysis of Xe, at lower pressures than used here, produces short-lived transient absorptions in the visible part of the spectrum.^{4,5} Similar absorptions have also been observed in solid rare gases exposed to electron pulses.^{6–8}

In this study of the pulse radiolysis of supercritical Xe we also observe a strong transient absorption, attributed to excimers.

An earlier study of liquid Xe, excited by high-energy electrons, reported that the VUV luminescence of the excimers could be quenched by application of an electric field.⁹ This showed that excimers are formed by recombination of precursor electrons and ions, which can be drawn out by the field (see eq 1).



There remained a fraction of the luminescence (25%) that was unaffected by the field, indicating approximately one-quarter of the excimers are formed directly.

This is an initial study of the pulse radiolysis of supercritical xenon. Xe has certain advantages, as indicated, and also interesting problems, like the formation of excimers, which complicate the detection of other transients by absorption spectroscopy. We show that this problem can be circumvented by adding small amounts of ethane. Initial results for electron transfer from C_6F_6^- to benzoquinone in supercritical Xe are presented. An interest is to see if the density augmentation around ions, which is known to occur,¹⁰ affects the rate, that is, to assess the effect of the observed increase in the radius of ions in the region of maximum compressibility on the rate of electron transfer. This augmentation represents a significant increase in the effective radius of the ions and also substantial solvent reorganization.

[†] Part of the special issue “Arnim Henglein Festschrift”.

Experimental Section

Chemicals. Xenon from MG industries (99.999%) was purified by passage through an "inert gas" Pall filter. Further purification was affected by irradiation with X-rays. Ethane from MG industries (scientific grade) was also passed through a C₂H₆ Pall filter. Hexafluorobenzene (99%) was from Aldrich. The *p*-benzoquinone (Aldrich 98%) was vacuum sublimed twice prior to use. All chemicals were degassed at 77 K on a vacuum line. Solutions were prepared by condensing a measured amount of vapor of the solute into the appropriate cell.

Cells. As described elsewhere,¹¹ the electrodes in the conductivity cell consist of thin Al films evaporated onto quartz plates. The temperature is read by a Pt thermometer mounted in the cell. A pressure transducer (Setra, model 212) is attached with readout in bar. Samples are condensed into the cell, which has a volume of approximately 50 cm³. The entire apparatus is thermostated during runs to ± 0.5 °C.

The cell used for transient absorption studies is made of 316 stainless steel. The internal volume is cylindrical (0.2 in. diameter) and 1 cm long. The ends are capped with Suprasil quartz windows, each 4 mm thick, held on with metal blocks and sealed with Ag-coated C-rings (EG&G Pressure Science). A pressure transducer is attached, and the temperature is read with a thermocouple in the steel block. The cell can be evacuated and pressurized through attached valves. This cell was pressure tested to 210 bar but is used routinely only to 150 bar.

Conductivity. For mobility and electron rate measurements, samples were irradiated using X-rays from either the 2 MeV van de Graaff, with pulses of 60–600 ns duration, or the Laser Electron Accelerator Facility (LEAF), with a 30 ps pulse. Typical doses are less than 10 μ Gy. The current signal is amplified with a current to voltage converter before being fed to either a transient recorder or oscilloscope (LeCroy 9362). Normally, the currents observed after the pulses measure the concentrations of electrons (n_e) so that the mobility can be determined from the drift time and rates of reaction can be determined from the current decay.

$$i = \frac{v_D e}{d} \int_0^d n_e(x, t) dx \quad (2)$$

The symbol d is the cell spacing. However as shown in eq 2, the current (i) is also a function of the drift velocity (v_D), and in Xe v_D changes with time after the pulse as the electrons thermalize. This gives rise to both positive and negative spikes on the nanosecond time scale.¹² In the presence of small amounts of ethane the current traces, obtained using LEAF, decay linearly at nanosecond times; that is, the spikes found in neat Xe at these times are removed by the addition of ethane.

Densities, viscosities, and compressibilities are determined using the NIST Database 12.¹³ It is assumed that the small amounts of ethane added (≤ 0.4 wt %) have negligible effect and the equation of state of xenon can be used.

Digitizer Transient Absorbance. Absorption spectra and kinetic information about transients are obtained at LEAF by transient absorption spectroscopy. The electron beam pulse passes through the cell windows and is stopped in a Faraday cup. Typical doses used in this study were from 1 to 10 Gy. Lower doses helped to slow the ion–ion recombination correction to the electron-transfer rates. The light from a pulsed high-pressure Xe lamp also passes through the windows but in the opposite direction. The light beam is brought out of the accelerator vault by mirrors and passes through interference filters of either 10 or 40 nm bandwidth. The signal is detected

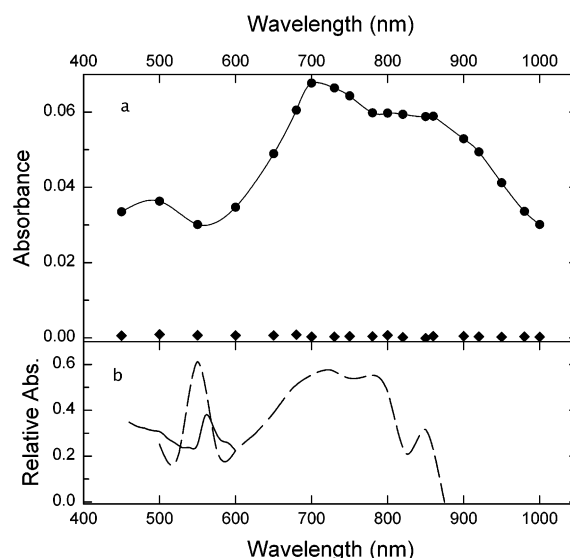


Figure 1. (a) Spectrum of transient formed in the pulse radiolysis of supercritical Xe at 79 bar: (●) absorbance at 1.8 ns; (◆) absorbance at 200 ns. (b) Spectra observed in Xe irradiated with 3 ns Febetron pulses: (---) at 3.1 bar;⁴ (—) at 25 bar.⁵

with a Si diode (FND-100) operated at -90 V. Signals are digitized with a 680B Tektronix oscilloscope, running on a DEC VAX station 4000 computer. The data are analyzed with Igor Pro software.

Pulse–Probe Transient Absorbance. The absorption of transients at picosecond times is done using an electron pulse and a variable time-delayed laser pulse at 800 nm. Typical doses were 1–3 Gy. Both beams traverse the cell in the same direction. The time response of the system using the 1 cm cell is about 15 ps. Details of this technique can be found elsewhere.¹⁴

Results

Xenon. Our results for the pulse radiolysis of supercritical xenon indicate that an intermediate is formed that absorbs quite strongly throughout the visible; Figure 1a shows the spectrum obtained at 79 bar. Similar results were obtained for other pressures in the range from 50 to 90 bar. The spectrum of this transient bears some similarity to the continuum spectrum, with a peak near 730 nm, reported earlier for Xe at 3.1 bar and shown in Figure 1b by the dashed line.⁴ Also shown by the solid line in Figure 1b is the absorption reported over a limited wavelength range for 25 bar Xe.⁵ This spectrum is normalized at 600 nm to that at 3.1 bar. The peak at 550 nm was not observed in our work. The broad absorption was attributed to excited dimeric species in the early studies. We roughly estimate that the extinction coefficient at the maximum is $1.9 \times 10^4 \text{ M}^{-1} \text{ cm}^{-1}$. This is based on the picosecond studies described below and assuming the yield of ions in supercritical Xe is the same as in the low-pressure gas, 4.57 per 100 eV.¹⁵ A similar yield was reported for liquid xenon.¹⁶

The assignment of this transient to excimer species is supported by the lifetime data derived from the decay of the absorption. The decay extends over 50 ns; by 200 ns the Xe sample is essentially transparent, as shown in Figure 1a. For a sample that had been extensively purified as described in the Experimental Section, the decay was found to be best fit by two first-order rates, eq 3.

$$A = A_S \exp(-k_1 t) + A_T \exp(-k_2 t) \quad (3)$$

TABLE 1: Lifetime and Yield of the Triplet Excimer

pressure, bar	density, g/cm ³	τ ns	$A_T/(A_S + A_T)^a$	ref
liquid		27		35
89.8	1.78	15.3	0.70	this work
66.6	1.42	21 ± 1	0.69	this work
49.7	0.426	31 ± 2	0.69	this work
29.5	0.195	39 ± 6	0.72	this work
1		100		30

^a Based on data for wavelengths between 660 and 860 nm.

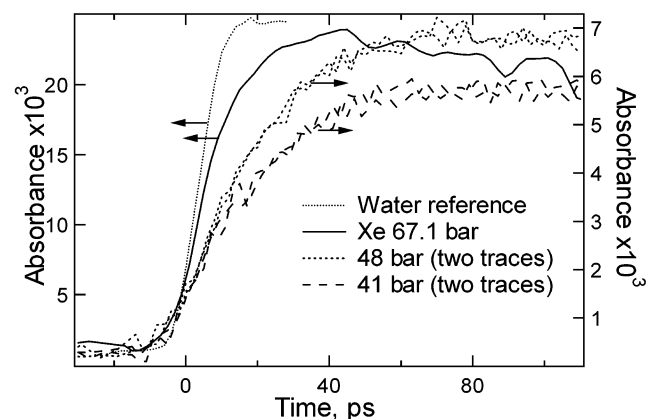


Figure 2. Growth of absorbance due to excimers in the pulse-probe experiment at 800 nm at various pressures: (approximate doses). (—) absorbance at 67.1 bar (3.0 Gy); (---) absorbance at 48 bar (0.94 Gy); (- - -) absorbance at 41 bar (0.82 Gy); (···) absorbance in a water sample (3.1 Gy).

This indicates there are two species, both of which absorb throughout the visible. One decays with a rate constant of $(1.9 \pm 0.4) \times 10^8 \text{ s}^{-1}$, independent of pressure, corresponding to a lifetime of 5.4 ns. This is in good agreement with the lifetime of the singlet excimer ($^1\Sigma_u^+$) of 4.3 ns reported for liquid xenon.¹⁷ The second component decays slower with pressure dependent lifetimes, as shown in Table 1, which are consistent with its identification as the triplet excimer ($^3\Sigma_u^+$). Also shown in Table 1 is the ratio of the initial absorbance of the triplet excimers (A_T) to the total initial absorbance ($A_S + A_T$). In the vicinity of the maximum this ratio is approximately 0.70.

Using the pulse-probe facility at LEAF allowed us to time resolve the formation of these excited species. We used an 800 nm probe beam and showed that the absorption grew in over a period of 100 ps at 41 bar and faster at higher pressures, as shown in Figure 2. As an indication of the overall time response of the experiment, a trace showing prompt absorbance in water due to the hydrated electron is included in Figure 2. The rates correlate well with expected rates for electron-ion recombination, reaction 1, the second-order rate constant which is given by the reduced Debye equation:

$$k_r = 4\pi e(\mu_+ + \mu_-)/\epsilon = 1.09 \times 10^{15}(\mu_+ + \mu_-)/\epsilon \text{ M}^{-1} \text{ s}^{-1} \quad (4)$$

This law of electron dynamics can safely be assumed to apply for mobilities (μ) up to 300 cm²/Vs. Deviations have been noted only in liquids where the mobility of the electron is higher.¹⁸ Calculated values of k_r for the conditions of the pulse-probe experiments are shown in Table 2. The mobility to use in eq 4 is that of the electron, because it is much greater than that of the positive ion. However μ_- is not known exactly at picosecond times when this recombination occurs. The mobility of thermal electrons at these densities is between 10 and 20 cm²/(V s),¹²

TABLE 2: Formation Rate of Excimers

pressure, bar	density, g/cm ³	[ion], μM	$k_r'(\text{obsd})$, s ⁻¹	$k_r, \text{M}^{-1}\text{s}^{-1}$		$\mu_-(\text{calcd})$, cm ² V ⁻¹ s ⁻¹
				obsd	calcd	
67.1	1.33	1.5	1.15×10^{11}	7.5×10^{16}	8.4×10^{16}	92
48.4	0.395	0.47	4.7×10^{10}	10.0×10^{16}	9.9×10^{16}	101
40.7	0.30	0.41	3.8×10^{10}	9.3×10^{16}	10.0×10^{16}	93

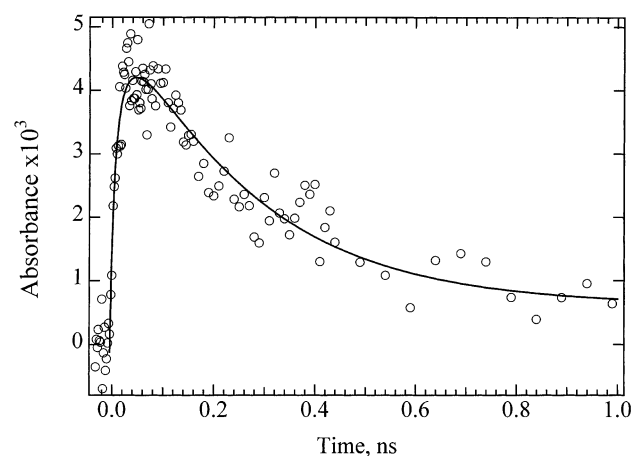


Figure 3. Decay of the absorbance due to excimer in the presence of 0.41% ethane: pulse-probe experiment at 800 nm; (O) absorbance at 49.2 bar, (—) fit to second-order growth, $k' = 6.8 \times 10^{10} \text{ s}^{-1}$, and first-order decay, $k = 3.85 \times 10^9 \text{ s}^{-1}$.

but the electrons are still hot at picosecond times. Mobility measurements at high electric fields, which cause the electrons to heat up indicate the mobility of hot electrons is much higher, between 60 and 100 cm²/(V s).^{10,19} The values of k_r , calculated by assuming a value of μ_- of 100 cm²/(V s), are shown in Table 2. Values of the bulk dielectric constant, ϵ , are those reported^{20a} for each density. The observed values of k_r were obtained by fitting the rise of the absorbance to a second-order rate expression and dividing the rate constant obtained, k_r' , by the ion concentration. The latter was derived using water as a dosimeter, and the yield of ions in supercritical xenon was assumed equal to the yield of solvated electrons in water, 4.8 per 100 eV.²¹ Corrections were made for electron density in calculating the dose. The good agreement of calculated and observed values of k_r indicates that the reason for the change in rate of growth of the excimer as the density decreases is that the concentration of ions decreases as the density decreases because the absorbed dose also decreases. Conversely, the observed pseudo-first-order decays can be used with the ion concentration to calculate the mobility of hot electrons. These results, shown in the last column of Table 2, indicate the mobility of hot electrons is around 100 cm²/(V s).

Xenon-Ethane Mixtures. The absorption due to excimers (Xe_2^*) presents a problem for pulse radiolysis kinetic studies because it obscures other transient absorptions. We found that adding ethane can quench the excimer. Our interest was to remove the excimer absorption at nanosecond times; 0.4 wt % ethane was sufficient for this purpose. The quenching rate was time-resolved in a pulse probe experiment, as shown in Figure 3. The solid line is a fit of the second-order growth and first-order decay. Analysis of the decay indicated the rate constant for quenching to be $(3.4 \pm 0.2) \times 10^{10} \text{ m}^{-1} \text{ s}^{-1}$ at pressures from 49 to 55 bar. The absorbance due to the excimers at nanosecond times was less than 0.001 with ethane present. Hexafluorobenzene also quenches the excimer species in Xe with a rate constant of $\approx (1.0 \pm 0.2) \times 10^{11} \text{ m}^{-1} \text{ s}^{-1}$. Similar but somewhat higher rates were reported for the quenching of

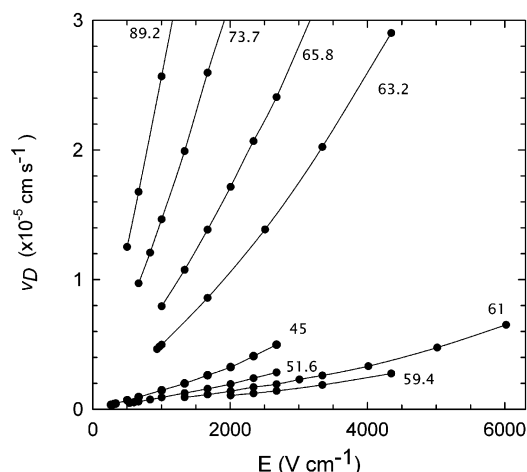


Figure 4. Drift velocity of electrons in xenon–ethane versus electric field at various pressures indicated (in bar) on graph.

TABLE 3: Electron Mobility and Thermalization Times in Xe Containing 0.4% Ethane At 20 °C

pressure, bar	density, g/cm ³	mobility, cm ² /Vs	τ_{TH} , ps
89.2	1.80	250	8.6
73.7	1.65	145	19.6
65.8	1.46	78.4	23.5
63.2	1.30	49.7	50.5
61.0	0.81	6.84	254
59.4	0.70	5.12	246
51.6	0.46	8.86	492
45.0	0.36	12.9	644

krypton excimers ($^3\Sigma_u^+$) by nitrogen and hydrogen near atmospheric pressure.²²

The addition of ethane has another effect, namely to provide scattering centers for electrons to lose energy faster. Thus hot electron effects are suppressed. This is important because electron reactions are energy dependent. For example, the rate of electron attachment to SF₆ in liquid xenon decreases as the electric field increases.²³ This was explained as an effect of the field that causes the electron kinetic energy to increase and the fact that the rate of this reaction is known to decrease with increasing electron energy.

The effect of ethane on the energy of the electrons was demonstrated in two ways. First, conductivity measurements on the nanosecond time scale showed no hot electron effects, as described in the Experimental Section; i.e., the current spikes disappeared. The second way, from measurements of the electron mobility, was more quantitative but less direct. Shown in Figure 4 is the drift velocity, v_D , of electrons versus field at various pressures in supercritical xenon. The linear region, from which the thermal electron mobility is obtained, extends to much higher fields than for neat xenon. Using eq 5,²⁴ we obtained the characteristic thermalization time, τ_{TH} , from E_{10} , the field at which v_D deviates 10% from linearity.

$$\tau_{TH} = \frac{3k_B T \ln[10(K_0/K_{TH} - 1)]}{20ne\mu_0 E_{10}^2} \quad (5)$$

where K is the kinetic energy of the electron, n the power dependence of v_D on E , and μ_0 the low field mobility. The values of n were between 1.1 and 1.4; K_0 was assumed to be 1 eV. The results in Table 3 show that a small amount of ethane reduces τ_{TH} from several nanoseconds in neat Xe to a few tens of picoseconds at the higher pressures. The thermalization time

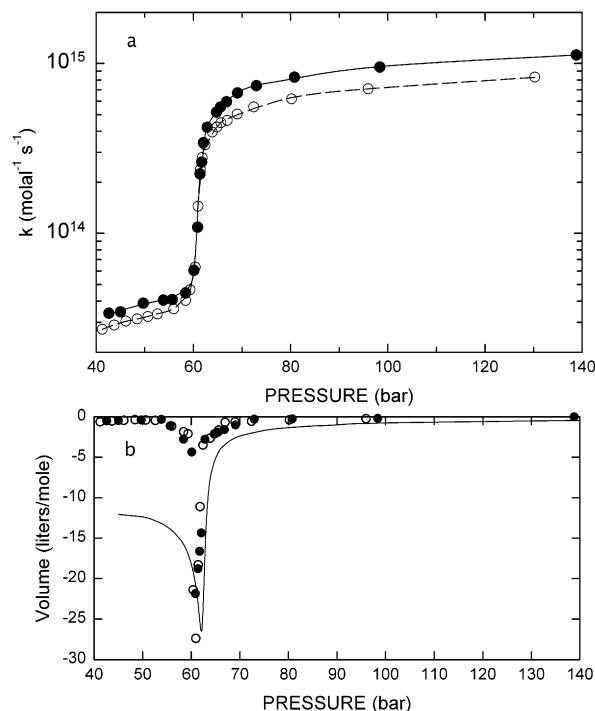
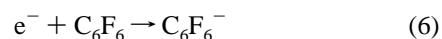


Figure 5. (a) Second-order rate constant for attachment to C₆F₆ in supercritical Xe containing 0.48% ethane as a function of pressure at 20 °C: (●) 3.0×10^{-9} M C₆F₆; (○) 6.2×10^{-9} M C₆F₆. Lines are least squares calculated fits. (b) Volume change for electron attachment to C₆F₆. Points are experimental activation volume obtained from the slope of the fitted curves in (a). The solid line is the volume of electrostriction around C₆F₆[−] calculated by the compressible continuum model.

does become longer as the pressure is reduced but remains below a nanosecond.

In contrast to the substantial effect of ethane on the thermalization of hot electrons, there is little or no effect of ethane on the thermal electron mobility. Values of μ_0 are obtained from the slopes of the curves in Figure 4 at low field. The results (see Table 3) show that the mobility is high at high pressure, decreases to a minimum value of 5 cm²/(V s) just below the critical density, and increases at lower densities, virtually the same behavior as in neat xenon. This result is similar to earlier reports that showed hydrocarbons at low concentrations have no effect on the low field mobility in liquid rare gases.^{25,26} As much as 5% CH₄ in liquid Kr does not affect the electron mobility.²⁶ Thus the addition of a small amount of ethane removes excess kinetic energy from hot electrons without changing drift mobilities, making the technique useful to study electron reactions by the nanosecond pulse conductivity method.

Electron Attachment to C₆F₆. (a) *Attachment Rates from Conductivity.* Attachment rates of electrons to C₆F₆ were measured by conductivity using X-ray pulses from the van de Graaff accelerator. Figure 5a shows the rate constant for reaction 6 as a function of pressure at 20 °C.



The rate constant is near $3 \times 10^{13} \text{ m}^{-1} \text{ s}^{-1}$ at low pressures, increases rapidly in the region of high compressibility around 62 bar, and levels off at about $1 \times 10^{15} \text{ m}^{-1} \text{ s}^{-1}$ at high pressure. The shape of the curve is similar to that obtained for electron attachment to NO in supercritical ethane¹¹ but the rate is much faster. Lines in Figure 5a are least squares quadratic fits over segments of the pressure range at a time.

(b) *Transient Absorption Results.* Hexafluorobenzene was chosen as a solute because it reacts rapidly with the electron in

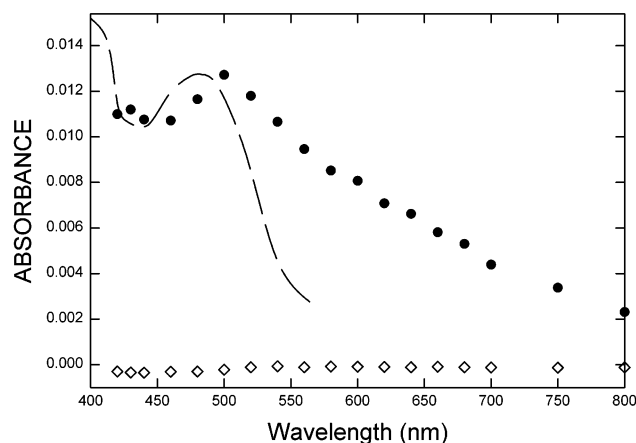


Figure 6. Transient spectrum in the pulse radiolysis of 66.2 bar Xe, containing 0.41% ethane and 1.5 mM C_6F_6 : (●) initial absorbance; (◇) final absorbance; (---) spectrum of $C_6F_6^-$ from literature (normalized).²⁷

Xe, as shown by the conductivity results. A large rate constant is necessary to compete with electron-ion recombination, which is fast as discussed above. Even at low pressures the rate is sufficient to capture electrons. Rate constants for attachment to CO_2 , C_2F_4 , and benzoquinone were determined by conductivity to be $<5 \times 10^{11} \text{ m}^{-1} \text{ s}^{-1}$. Therefore millimolar concentrations of these solutes would be unsuitable and would not compete for the electron with recombination.

The spectrum obtained in the pulse radiolysis of a 1.5 mM solution of C_6F_6 in the xenon-ethane mixture at 66 bar and 25 °C is shown in Figure 6. This spectrum resembles that obtained for $C_6F_6^-$ in 2,2,4,4-tetramethylpentane solvent,²⁷ shown by the dashed lines and that obtained in 2,2,4-trimethylpentane solutions;²⁸ however, it is slightly red shifted and considerably broadened in the supercritical media. This spectrum has been normalized to the absorbance at the peak for $C_6F_6^-$ in xenon-ethane for comparison purposes. The broadening suggests that the extinction coefficient (ϵ) of $4500 \text{ M}^{-1} \text{ cm}^{-1}$ at 486 nm reported by Sowada and Holroyd may not be valid here and that a lower value should be used. We estimate a value of $\epsilon = 2800 \pm 200 \text{ M}^{-1} \text{ cm}^{-1}$ at 500 nm, using the solvated electron yield in water for dosimetry, assuming $G(e_{aq}^-) = 2.75$ for nanosecond times, and correcting for electron density in the samples.

In nonpolar liquids $C_6F_6^-$ anions are known to form dimer ions.²⁸ This reaction is minimized at the concentration of hexafluorobenzene used here. That these ions disappear largely by ion recombination is supported by the kinetics, which exhibit second-order decay, and by the dose dependence. As shown in Figure 1S, the pseudo-first-order rate constant k_r' increases linearly with dose. Lower rates and longer lifetimes of the $C_6F_6^-$ anions were observed when lower charges were used in the accelerator pulses.

At 66 bar an initial lifetime of 53 ns was found for an average charge of $4.3 \pm 0.2 \text{ nCoulombs}$ in the pulse. Because the initial concentration of $C_6F_6^-$ was $4.2 \mu\text{M}$, on the basis of the derived value of the extinction coefficient, ϵ , this corresponds to a second-order rate constant of $4.4 \times 10^{12} \text{ M}^{-1} \text{ s}^{-1}$. At the pressure of the experiment, 66.1 bar, the sum of the mobilities is $3.45 \times 10^{-3} \text{ cm}^2/(\text{V s})$ (see next section and ref 10) and the dielectric constant, ϵ , is 1.25.^{20a} The calculated recombination rate constant from eq 4, using these values, is $3 \times 10^{12} \text{ M}^{-1} \text{ s}^{-1}$. The high yield of free ions mentioned in the Introduction is advantageous in that high concentrations of solute ions can be formed, but disadvantageous in that ion recombination is

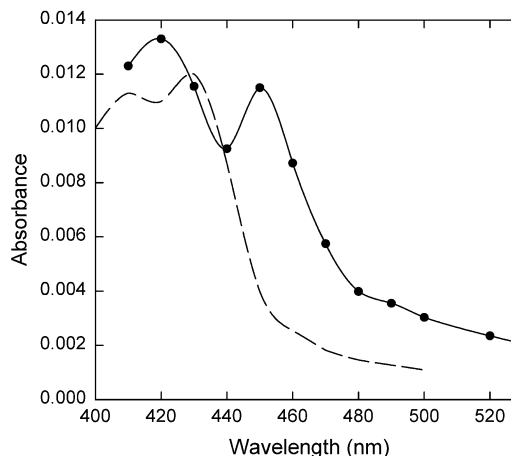


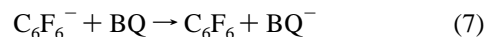
Figure 7. (Solid line) transient spectrum obtained at 60 ns for a solution containing 4 mM C_6F_6 and 0.8 mM benzoquinone at 65.2 bar Xe. (Dashed line) spectrum reported for BQ^- in aqueous solution.²⁹

then quite fast. At lower pressures lower concentrations of ions are formed because the absorbed dose is less; however, the mobility of the ions increases with decreasing pressure; that is, the product $[\text{ion}]k_r$ is approximately constant, and the net result is the ion lifetimes show little change with pressure. Lowering the pressure from 66 to 59 bar, which caused a 35% density decrease, left the recombination rate essentially the same.

Mobility of $C_6F_6^-$. The mobility of $C_6F_6^-$ was measured in the xenon-ethane mixture from the drift time of the anions. Electrons are rapidly captured by the hexafluorobenzene at the concentration used, $14 \mu\text{M}$, so that the drift is entirely attributable to the anions. Two ion drift times were apparent at most pressures. Because anions generally have higher mobilities than positive ions,^{20b} this was assumed to be the case here. The mobility of $C_6F_6^-$ at 21.4 °C is $1.2 \times 10^{-3} \text{ cm}^2/(\text{V s})$ at 146 bar and increases with decreasing pressure, as shown in Table S-1. The results are similar to those for the positive ion in xenon.¹⁰ In the critical region, near 62 bar, the mobility is $2.3 \times 10^{-3} \text{ cm}^2/(\text{V s})$, which is slightly greater than that of the positive ion. These mobilities were used to calculate the diffusion coefficient and radius of the negative ion.

Electron Transfer from $C_6F_6^-$ to BQ. The addition of benzoquinone to either xenon or xenon-ethane containing hexafluorobenzene causes a faster decay in the 500 nm region and a grow-in at 440 nm. The decay around 500 nm is first order. The spectrum at short times is similar to that of $C_6F_6^-$ shown in Figure 5; the spectrum at 60 ns is shown in Figure 7. This resembles that reported for BQ^- in aqueous solution with a maximum at 430 nm.²⁹ In the supercritical fluid there is a small red shift. Spectra were similar in xenon and xenon-ethane solvents.

The kinetics of electron transfer for the reaction



were studied in the xenon-ethane mixture to avoid interference by the excimer absorption. The rate of reaction 7 was determined from the disappearance of $C_6F_6^-$ monitored at 520 to 540 nm. This decay was first order in the presence of BQ. In the absence of BQ the decay was second order and dose dependent as described above. To calculate the rate constant, k_7 , corrections were made for the decay in the absence of BQ. This correction was less at the lower doses. The results are shown by the points in Figure 8a; the units for the rate constant, k_7 , are $\text{mol}^{-1} \text{ s}^{-1}$. The rate constant shows a maximum at 62 bar.

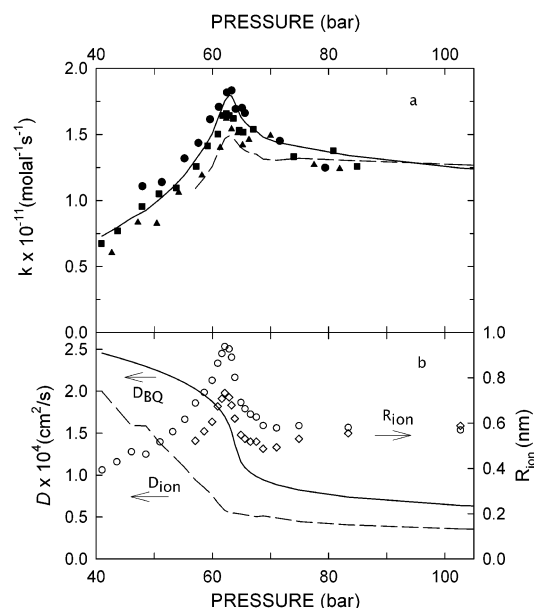


Figure 8. (a) Rate constant for electron transfer from C_6F_6^- to BQ versus pressure. Experimental: (●) 0.28 mM BQ; (■) 0.25 mM BQ, (▲) 0.34 mM BQ. Lines calculated by eq 11: (---) using HCC radius; (—) using radius from Stokes' eq 12. (b) Values of parameters: D_{ion} (—), D_{BQ} (---), and R_{ion} (◇) HCC calculation. (○) Stokes' equation as a function of pressure.

Discussion

Excimers. Our lifetime data based on the absorbance decay (see Table 1) shows that the lifetime of the longer lived species is pressure dependent. The lifetime of the triplet excimer ($^3\Sigma_u^+$), measured by emission of the excimer at 178 nm,³⁰ showed a similar pressure dependence. Both the absorption and luminescence data gave the same lifetime for the shorter lived species, the singlet excimer ($^1\Sigma_u^+$). Thus the transient absorption is attributed to these excimers. If the extinction coefficients for triplet and singlet are the same at 700 nm, the excimers are 70% triplet. Triplets are expected to dominate because, as discussed above, they are formed by volume recombination and random recombination leads to 75% triplet states.³¹

Electron Attachment to C_6F_6 . The rate constant for attachment to C_6F_6 at high pressure is quite large. Warman³² has pointed out that electron attachment rates are not expected to exceed a value of about $3 \times 10^{14} \text{ M}^{-1} \text{ s}^{-1}$. Values for attachment to SF_6 generally level off near this value when the electron mobility is high. An apparent exception is attachment to SF_6 in liquid methane where the rate constant is $9 \times 10^{14} \text{ M}^{-1} \text{ s}^{-1}$,³³ the highest value known for a liquid. In the same units our value at the highest pressure is $5.6 \times 10^{14} \text{ M}^{-1} \text{ s}^{-1}$, slightly above Warman's maximum limit. However, this value is an order of magnitude below that expected if the rate constant were given by the diffusion rate

$$k_D = 4\pi R \mu_B T \rho N / 1000 \quad (8)$$

if the radius, R , is taken as 1 nm and ρ is the density. Equation 8 gives a value of $2.3 \times 10^{16} \text{ M}^{-1} \text{ s}^{-1}$ at 139 bar.

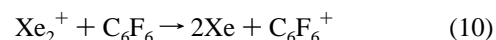
The activation volume for reaction 6 was calculated from the derivative of the fitted curves in Figure 5a and the relation

$$V_a^* = -RT \partial(\ln k_a) / \partial P \quad (9)$$

The results are shown in Figure 5b. The activation volumes are generally on the order of -1 to -2 L/mol except in the region

of high compressibility. At the minimum V_a^* is -28 L/mol . Also shown in the figure are volumes of electrostriction, V_{el} , for the C_6F_6^- ion calculated by the compressible continuum model.¹¹ The full electrostriction volume would not be expected until the reaction is complete. However, there is good agreement of V_{el} with V_a^* above 62 bar. There is no agreement at lower pressures. Thus the transition state is close to the reactants at low pressure but close to the products at high pressure.

The transient formed in the presence of C_6F_6 is assigned to the anion on the basis of agreement with known spectral data. The cation of C_6F_6 could also contribute to the absorption because the capture of electrons by C_6F_6 will increase the lifetime of Xe_2^+ . The reaction



is energetically feasible on the basis of the ionization potential of C_6F_6 , which is 10 eV,²⁸ and that of xenon dimer is 11 eV.⁴ The cation C_6F_6^+ is reported to absorb at 450 nm but has only a small absorption at 500 nm in a matrix at 77 K.³⁴ However, we did not observe a peak near 450 nm. Also, the formation of C_6F_6^+ will depend on the rate constant for reaction 10. If it is comparable to the rate of electron transfer reported below we do not expect this ion will make a significant contribution to at least the initial absorption.

Electron Transfer. The rate of electron transfer from C_6F_6^- to benzoquinone is fast. The rate constant is in excess of $1 \times 10^{11} \text{ m}^{-1} \text{ s}^{-1}$ at most pressures at 21 °C. We compare the observed results with the rate expected for a diffusion-controlled reaction; in which case the rate constant should be given by

$$k_D = 4\pi(R_{\text{ion}} + R_{\text{BQ}})(D_{\text{ion}} + D_{\text{BQ}})\rho N / 1000 \text{ m}^{-1} \text{ s}^{-1} \quad (11)$$

It is assumed that the values of R_{ion} to use in eq 11 are those of the clustered ions, as calculated from the mobilities using either the hydrodynamic compressible continuum model,¹⁰ which takes the distance dependence of the density and viscosity, η , into account, or the Stokes' equation (12) and values of the macroscopic viscosity. The values of D_{ion} used are also obtained from the measured mobilities and the Einstein relation $D_{\text{ion}} = \mu_{\text{ion}} k_B T / e$. These values are given in Table S-1 or Figure 8b.

$$R_{\text{ion}} = e / 6\pi\eta\mu_- \quad (12)$$

The radius used for the neutral BQ is that obtained from the molar volume, 0.32 nm. With this radius, together with viscosity data, values of D_{BQ} were derived from the Stokes–Einstein equation:

$$D_{\text{BQ}} = kT / 6\pi\eta R_{\text{BQ}} \quad (13)$$

These parameters and eq 11 were used to predict the rate constants shown by the lines in Figure 8a. A peak in the rates is predicted in the region of maximum compressibility. This peak is attributed to clustering around the reacting anion, leading to larger values of R_{ion} at this pressure. A good agreement is obtained using the value of R_{ion} calculated with Stokes' equation. At all pressures $D_{\text{BQ}} > D_{\text{ion}}$, and $R_{\text{ion}} > R_{\text{BQ}}$, both inequalities can be attributed to the large cluster around the ion.

In summary, it is shown that the addition of a small amount of ethane effectively quenches excimer absorption and makes the observation of transient species possible. The observed electron-transfer rate from C_6F_6^- to benzoquinone is comparable to that calculated for diffusion and shows the same pressure dependence. The maximum in the rate near 62 bar provides

additional evidence of the formation of clusters around ions, which has been demonstrated previously for Xe by ion mobility studies¹⁰ and for ethane by electron equilibria studies.³⁶ Further studies are needed to see if this interesting pressure dependence of the rate constant will be observed in other charge-transfer reactions in supercritical fluids.

Acknowledgment. We thank Andy Cook, John Miller, Allison Funston, Steve Howell, J. P. Kirby, and Pavel Poliakov for help with experiments at LEAF. Special thanks to C. Koehler and J. Anselmini for technical assistance. This research was carried out at Brookhaven National Laboratory and supported under contract DE-AC02-98-CH10886 with the U.S. Department of Energy and supported by its Division of Chemical Sciences, Office of Basic Energy Sciences. K.I. and M.N. are supported by a grant from the Japanese Society for the Promotion of Sciences under Japan-U.S. Cooperative Science Program, Joint Research.

Supporting Information Available: Table of mobility, radius, and diffusion coefficient data and a graph of rate constant vs dosage. This material is available free of charge via the Internet at <http://pubs.acs.org>.

References and Notes

- (1) Dimitrijevic, N. M.; Takahashi, K.; Bartels, D. M.; Jonah, C. D.; Trifunac, A. D. *J. Phys. Chem. A* **2000**, *104*, 568–576.
- (2) Shkrob, I. A.; Sauer, J. M. C. *J. Phys. Chem. B* **2001**, *105*, 4520–4530.
- (3) Takahashi, K.; Jonah, C. D. *Chem. Phys. Lett.* **1997**, *264*, 297–302.
- (4) Killeen, K. P.; Eden, J. G. *J. Chem. Phys.* **1986**, *84*, 6048–6074.
- (5) Zamir, E.; Huestis, D. L.; Nakano, H. H.; Hill, R. M.; Lorents, D. C. *IEEE J. Quantum Electron.* **1979**, *QE-15*.
- (6) Suemoto, T.; Kondo, Y.; Kanzaki, H. *Solid State Commun.* **1978**, *25*, 669–672.
- (7) Dossel, O.; Nahme, H.; Haensel, R.; Schwentner, N. *J. Chem. Phys.* **1983**, *79*, 665–670.
- (8) Nahme, H.; Schwentner, N. *Appl. Phys. B* **1990**, *51*, 177–191.
- (9) Kubota, S.; Nakamoto, A.; Takahashi, T.; Hamada, T.; Shibamura, E.; Miyajima, M.; Masuda, K.; Doke, T. *Phys. Rev. B* **1978**, *17*, 2762–2765.
- (10) Itoh, K.; Holroyd, R. A.; Nishikawa, M. *J. Phys. Chem. A* **2001**, *105*, 703–709.
- (11) Nishikawa, M.; Holroyd, R.; Itoh, K. *J. Phys. Chem. B* **1998**, *102*, 4189–4192.
- (12) Holroyd, R. A.; Itoh, K.; Nishikawa, M. *J. Chem. Phys.* **2003**, *118*, 706–710.
- (13) Friend, D. G. "NIST Thermophysical Properties of Pur Fluids, version 3.0 Database 12," NIST, 1992.
- (14) Wishart, J. F. In *Studies in Physical and Theoretical Chemistry*; Jonah, C. D., Rao, B. S. M., Eds.; Elsevier Science: Amsterdam, 2001; Vol. 87, pp 21–35.
- (15) Srdoc, D.; Inokuti, M.; Krajcar-Bronic, I. *Atomic and Molecular Data for Radiotherapy and Radiation Research*; International Atomic Energy Agency: Vienna, Austria, IAEA-TECDOC-799, 1995.
- (16) Huang, S. S.-S.; Freeman, G. R. *Can. J. Chem.* **1977**, *55*, 1838–1846.
- (17) Hitachi, A.; Takahashi, T.; Funayama, N.; Masuda, K.; Kikuchi, J.; Doke, T. *Phys. Rev. B* **1983**, *27*, 5279–5285.
- (18) Nakamura, Y.; Shinsaka, K.; Hatano, Y. *J. Chem. Phys.* **1983**, *78*, 5820–5824.
- (19) Holroyd, R. A. Unpublished.
- (20) Schmidt, W. F. *Liquid-State Electronics of Insulating Liquids*; CRC Press: Boca Raton, 1997; (a) p 19, (b) p 119.
- (21) Pimblott, S. M.; LaVerne, J. A.; Bartels, D. M.; Jonah, C. D. *J. Phys. Chem.* **1996**, *100*, 9412–9415.
- (22) Ito, Y.; Arai, S. *Bull. Chem. Soc. Jpn.* **1984**, *57*, 3062–3065.
- (23) Sowada, U.; Bakale, G.; Yoshino, K.; Schmidt, W. F. *Chem. Phys. Lett.* **1975**, *34*, 466–469.
- (24) Warman, J. M. *Radiat. Phys. Chem.* **1981**, *17*, 81.
- (25) Sowada, U.; Schmidt, W. F.; Bakale, G. *Can. J. Chem.* **1977**, *55*, 5.
- (26) Borghesani, A. F.; Folegani, M.; Frabetti, P. L.; Piemontese, L. *J. Chem. Phys.* **2002**, *117*, 5794–5801.
- (27) Sowada, U.; Holroyd, R. A. *J. Phys. Chem.* **1980**, *84*, 1150–1154.
- (28) van den Ende, C. A. M.; Nyikos, L.; Warman, J. M.; Hummel, A. *Radiat. Phys. Chem.* **1982**, *19*, 297–308.
- (29) Willson, R. L. *Trans. Faraday Soc.* **1971**, *67*, 3020.
- (30) Morikawa, E.; Reininger, R.; Gurtler, P.; Saile, V.; Laporte, P. *J. Chem. Phys.* **1989**, *91*, 1469–1477.
- (31) Brocklehurst, B. *Radiat. Phys. Chem.* **1997**, *50*, 213–225.
- (32) Warman, J. M. In *The Study of Fast Processes and Transient Species by Electron Pulse Radiolysis*; Baxendale, J. H., Busi, F., Eds.; Reidel: Dordrecht, Holland, 1982; p 433ff.
- (33) Bakale, G.; Sowada, U.; Schmidt, W. F. *J. Phys. Chem.* **1975**, *79*, 3041–3044.
- (34) Shoute, L. C. T.; Mittal, J. P. *Radiat. Phys. Chem.* **1987**, *30*, 105–111.
- (35) Kubota, S.; Hishida, M.; Raun, J. *J. Phys. C* **1978**, *11*, 2645–2651.
- (36) Holroyd, R. A.; Nishikawa, M.; Itoh, K. *J. Phys. Chem. B* **2000**, *104*, 11585–11590.